This paper is available online at www.praiseworthyprize.org
International Review of Aerospace Engineering (I.RE.AS.E), Vol. 14, N. 4
ISSN 1973-7459
August 2021

Numerical Study of the Main Rotor Wake Structures and Induced Velocity Fields at the Tail Rotor Location When Flying Near the Ground

Yuri M. Ignatkin[1], Pavel V. Makeev[1], Alexander I. Shomov[1], Valery A. Ivchin[2]

Abstract – *This paper considers the Mi-8 helicopter main rotor aerodynamics when flying near the infinite ground surface. The research is based on the free wake model developed by authors at Moscow Aviation Institute. The distance from the rotor's hub to the ground surface in the range of H = 6-16 m and the values of free stream (flight) velocity in the range of V = 0-15 m/s are considered. The results of the visualization for both rotor wake shapes and streamlines are obtained. The influence of the ground proximity on the rotor wake shape, including the formation of "supervortex" and "ground vortex" structures are analyzed. The induced velocity fields of the main rotor in the area of the tail rotor location for various azimuth positions relative to the main rotor axis are studied. The conclusion is made about the significant influence of the ground effect on the rotor wake structure and induced velocities field, including the area of the tail rotor location. Particularly, at slip flight with speed V = 10 m/s, when the distance to the ground surface H increases from 6 to 12 m, the value of the average induced velocity at the tail rotor plane is growing up to four times. The obtained data have allowed taking into account such effects of aerodynamic interference in the simplified mathematical model of the research flight simulator of JSC Helicopters Mil and Kamov.*

Keywords: *Main Rotor, Free Wake Model, Hover, Forward Flight, Ground Effect, Tail Rotor Location, Induced Velocities*

Nomenclature

ρ	Air density [kg/m^3]
t	Time [s]
R	Rotor radius [m]
α_R	Angle of attack of a rotor [°]
β	Angle of slip [°]
N_b	Number of blades
c	Blade chord [m]
σ	Rotor solidity, $N_b c/\pi R$
θ_{tw}	Blade twist [°]
θ	Blade pitch angle [°]
ωR	Rotor blade tip speed [m/s]
n	Number of revolutions of a rotor
V	Free stream (flight) velocity [m/s]
T	Rotor thrust [N]
Q	Rotor torque [N m]
c_T	Rotor thrust coefficient $(2T)/(\rho(\omega R)^2\pi R^2)$
c_Q	Rotor torque coefficient $(2Q)/(\rho(\omega R)^2\pi R^3)$
H	Distance between rotor hub and ground surface [m]
ψ	Tail rotor plane position relative to the main rotor axis [°]

I. Introduction

The helicopters main rotor aerodynamics at the forward flight (or in hover under wind conditions) has its own features, including the ones related to the formation of the rotor wake structure [1]. Already at low speeds of the incoming flow (advance ratio μ = 0.025-0.05) the vortex wake shape transforms from the cylindrical to a much more complex shape due to the mutual influence of the vortices. As a result of rolling up the edges of the vortex wake, new vortex structures are formed, with localization in the form of right and left "supervortexes".

These "supervortexes" determine the main part of the induced velocities around the rotor. As the research result shows, in the range of values μ = 0.05-0.1, these "supervortexes" have the highest power. This issue has been previously investigated by the authors (Ignatkin et al., 2018) [2], 2020 [3]). The main rotor wake has an even more complex structure at low speeds (or in hover under wind conditions) in ground effect. In this case, the vortex wake may differ significantly from the wake of a rotor out of ground effect (under free stream), Phillips (2010) [4]. For a single-rotor helicopter scheme, the features of main rotor's wake structure in forward flight are of high importance. Under certain conditions, the tail rotor can fall under the high-induced influence of the

Available online by August 31st, 2021
https://doi.org/10.15866/irease.v14i4.19744

main rotor. This is possible when flying with a slip, or when hovering under the wind conditions. In particular, the work by Fletcher & Brown (2010) [5], the work by Ignatkin et al. (2014) [6] and the work by Arda and Yüksel (2019) [7] have been focused on the computational study of the main and tail rotor interference. These works consider flying modes with the slip for the free stream conditions out of ground effect. A possible reduction of the tail rotor aerodynamic characteristics due to interference can lead to an increase in its power consumption and a decrease in the efficiency of control.

These issues need to be studied and taken into account not only when designing the helicopters, but also when developing software that simulates the helicopters' aerodynamics and flight dynamics as a part of flight simulators. The study of the helicopter rotor aerodynamics in ground effect can be carried out both by experimental research and numerical modeling.

Experimental studies of the aerodynamic characteristics of helicopter rotors in hover and forward flight near the ground surface in wind tunnels are associated with large material and time costs, as well as significant technical difficulties. Earlier experimental work in this area has been mainly focused on the analysis of the influence of the ground surface on the aerodynamic characteristics of the rotor, such as the work by Knight and Hefner (1941) [6] and Cheeseman and Bennett (1957) [9]. Koo and Oka (1971) [10] also present the results of the flow structure study around a rotor operating near the ground. The article by Sheridan and Wiesner (1977) [9] provides an overview of the work carried out by Boeing-Vertol Company. Much attention in these studies is paid to the visualization of the rotor wake structure at the low speeds in ground effect. The phenomenon of a "ground vortex" that occurs due to the rolling-up of the leading edge of the rotor wake has been analyzed. Light (1989) [12] has analyzed the geometry of the rotor wake by visualizing the rotor blade tip vortices. A research conducted by Borisov et al. (2015) at TsAGI [13] has been focused on the influence of limited ground surface on the characteristics of the rotor in hover. Qualitative analysis of the flow structure around the rotor in ground effect has been made possible with the development of PIV (particle image velocimetry) methods. Such studies have been carried out in the works by Lee (2008) [14] and Nathan & Green. (2011) [15]. Much attention in these works has been paid to the phenomenon of the "ground vortex". The PIV method has allowed analyzing the velocity fields and constructing the streamlines. The possibilities of numerical modeling of rotor aerodynamics at the low flight speeds have been limited for a long time by the lack of computational resources. In recent years, the development of computer technology has made this possible. At the same time, it should be noted that modeling the aerodynamic characteristics of a helicopter's rotors is still one of the most complex and resource-intensive tasks in this area. Numerical methods for modeling fluid dynamics, known as CFD (computational fluid dynamics) methods, are currently represented by several areas used in helicopter rotor aerodynamics problems. Various vortex methods are widely applied. Modern vortex models represent a vortex wake behind the rotor blades in unsteady and nonlinear settings. This allows accurate modeling of the field of induced velocities around the rotor. Vortex models are used to solve problems of rotor aerodynamics in ground effects in such works as [16]-[18]. The work by Griffiths et al. (2002) [16] is based on the vortex model FWM (Free Wake Model) and it considers a combination of two rotors in ground effect. The work by Zhao & He (2014) [17] is based on the VPM (Vortex Particle Method) method and considers various issues of main and tail rotors' aerodynamics, covering the mutual aerodynamic interference in ground effect. The work by Aparinov et al. (2017) [18] has also used a vortex model and it is focused on the study of helicopter rotor aerodynamics near a limited ground surface (ship's helideck). An important advantage of vortex models is their relatively low requirement for computing resources.

Conventional personal computers are sufficient for their use. In addition to the works mentioned above, the work by Pasquali et al. (2020) [19] can be noted. It is based on the original BEM (boundary element method) solver. This paper presents the results of studies of the aerodynamic characteristics of the rotor at hover in ground effect for cases of parallel and inclined ground surfaces. Two approaches to model the ground surfaces are used: mirrored wake and bound domain method.

Recently, CFD methods based on the numerical solution of Navier-Stokes equations with the Finite Volume Method (FVM) and various turbulence models have also been widely used for modeling rotor aerodynamics [30], [31]. In order to solve such problems, the Unsteady RANS (Reynolds Averaged Navier Stokes) approach is used most often. An example of such papers can be the works [20]-[26], [32]. The article by Kutz et al. (2012) [20] considers rotor in hover near the ground surface based on the FLOWer CFD package developed in DLR. The work by Sugiura et al. (2017) [21] examines the forward flight of a rotor-fuselage combination in ground effect based on two different CFD packages: HMB3 (Helicopter Multi-Block) solver developed at the University of Glasgow and CFD solver developed at the Japan Aerospace Exploration Agency. The work by Salini et al. (2019) [22] analyzes the rotor aerodynamics in hover near the ground based on several approaches, including the original CFD-solver RotCFD. The work by Şahbaz et al. (2019) [23] considers an isolated rotor in hover near an inclined ground surface. In the work by Rovere et al. (2019) [24], based on HMB3-solver, the performance of small-size and large-size rotors in hover in ground effect has been studied. This research has been also focused on the study of the flow around the rotors.

Wang's et al. paper (2019) [25] is dedicated to the modeling of the aerodynamic characteristics of a rotor when flying near the ground surface for three cases:

infinite ground surface effect, finite ground surface effect, and finite ground surface effects with different blocked area. In the work by Silva et al. (2021) [26], the FVM based on Multiple Reference Frame (MRF) technique is used to simulate the aerodynamic characteristics of a hovering rotor in ground effect. A large number of works on numerical modeling of helicopter rotor aerodynamics in ground effect has also been performed based on the VTM (vorticity transport model) model of Brown [4], [27]. In particular the dissertation work by Phillips (2010) [4] deals with many issues of rotor aerodynamics in ground effect, including a single rotor and a two-rotor tandem scheme. It is worth noting that the large number of results of rotor flow visualization in ground effect was obtained by Phillips.

Summarizing the possibilities of numerical methods for modeling rotor aerodynamics in ground effect, it should be noted that today CFD methods based on FVM are still very resource-intensive. This is especially true for low-speed flight modes, where it is necessary to simulate a large number of rotor revolutions. The practical application of such methods requires the use of high-performance supercomputer clusters. However, it is difficult to perform parametric calculations for a large number of operating modes. In this regard, vortex methods remain very relevant for solving such problems.

The presented work is focused on the numerical modeling of aerodynamics of isolated Mi-8 helicopter's main rotor in ground effect. The free wake model [28] developed at Moscow Aviation Institute is used.

The first part of the article contains descriptions of the used numerical model. The next part is dedicated to investigations of the rotor performance at hover in/out of ground effect. The obtained data have been verified by comparing the results of the experimental and the computational studies by other authors. The final (main) part of the article is dedicated to the research of the rotor performance at the forward flight in ground effect. The vortex wake shapes, the flow images and the diagrams of the averaged induced velocities in the tail rotor location area have been obtained and analyzed.

II. Method and Object of Study

II.1. Free Wake Model of a Rotor

The free wake model of the rotor [28] developed at the Helicopter Design Department of Moscow Aviation Institute is based on the lifting line theory and the blade element theory. Each blade element is modeled by an attached vortex segment located on a quarter of the blade element chord c (Fig. 1) with the control point in the center of the segment. In each time step Δt, a quadrangular contour consisting of vortex segments with a constant circulation Γ, equal to the attached vortex circulation, descends from the blade element. The circulation of the attached vortex changes along the blade radius and depends on the blade azimuthal position. The system of vortex contours creates a free vortex wake in the form of a grid of longitudinal and transverse vortex segments (Fig. 1). The vortex wake grid is deformed at each calculated step under the influence of external and induced velocity fields. The circulation of the attached vortex of the blade element is calculated with coupling equation:

$$\Gamma = 0.5 C_L W c \tag{1}$$

The coefficients of the lift force C_L and the drag force C_D of the blade element are determined at the found angle of attack α and the total flow velocity W based on airfoil steady test data in wind tunnel. The attached vortex circulation is determined with an iterative method.

A key part of the considered model is the calculation of induced velocities from the vortex segment, which is an element of the free vortex trace behind the rotor. The described model uses an approach that allows determining the vorticity field from the vortex segment and the induced velocity from this vorticity field based on an exact solution of the vortex source diffusion [28].

The vorticity of the vortex segment of length L taking into account its diffusion is determined by the equation:

$$\vec{\omega} = \frac{\Gamma}{16(\pi \nu t)^{\frac{3}{2}}} \times \int_L \mathrm{e}^{-\frac{r^2}{4\nu t}} d\vec{l} \tag{2}$$

Here Γ is the circulation, ν is the coefficient of kinematic viscosity, r is the distance from the center of the segment, t is the diffusion time (Fig. 2).

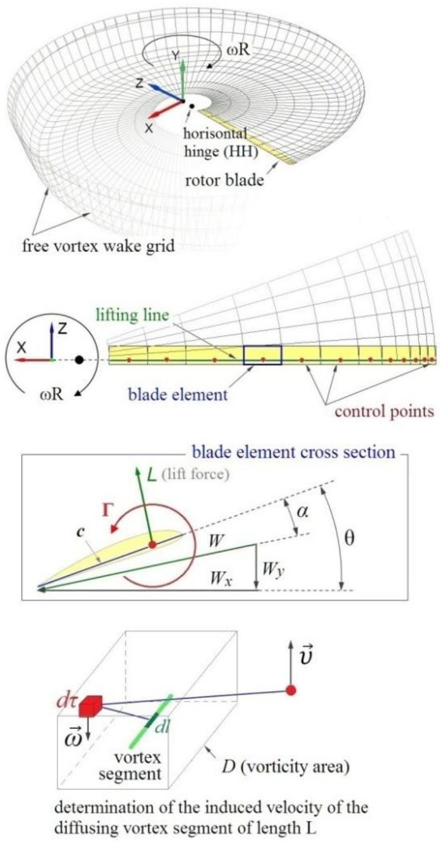

Fig. 1. Free wake model

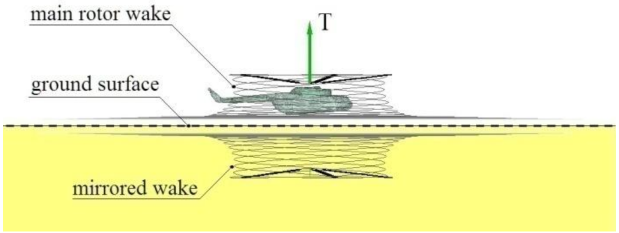

Fig. 2. Computational model of the Mi-8 helicopter main rotor in ground effect

The induced velocity $\vec{v}$ of the vortex segment length L can be determined by the equation:

$$\vec{v} = \frac{1}{2\pi} \times \iiint_D \frac{\vec{\omega} \times \vec{r}}{r^3} d\tau \tag{3}$$

Here D is the the area where the vorticity field is calculated, $d\tau$ is the the elementary three-dimensional volume and r is the the distance from the velocity calculation point to the point in the vorticity field.

Integral (Eq. (2)) does not have an analytical solution in finite limits. The numerical solution of the integral (Eq. (3)) will lead to a large computing resources costs.

In order to reduce the calculation time, pre-calculated tables of induced velocities from a normalized vortex segment are used, depending on the length of the segment L, the degree of its diffusion (time t), and the distance r from the segment to the point.

The free wake model provides the determination of the aerodynamic characteristics of single rotor and various multi-rotor configurations with the aerodynamic interference.

II.2. Computational Model of the Main Rotor of the Mi-8 Helicopter in Ground Effect

The characteristics for the Mi-8 main rotor are given in [29] and are presented in Table I. The main rotor has five rectangular blades with NACA 230-12 airfoil, each one modeled by 12 calculation elements. The rotor blade is modeled as absolutely rigid for bending and torsion.

The flapping movement relative to the horizontal hinge is taken into account.

The influence of the ground surface is considered by the mirrored wake method (Fig. 2), which is popular and accurate [19] for modeling ground effect for case of infinity surface. The Mi-8 fuselage in Fig. 2 and onwards is shown symbolically and it has been excluded from computational modeling.

TABLE I
PARAMETERS OF THE MAIN ROTOR UNDER STUDY

Components	Name	Value
R	Rotor radius	10.65 m
ωR	Rotor blade tip speed	214 m/s
N_b	Number of blades	5
σ	Rotor solidity	0,0777
c	Blade chord	0.52 m
θ_{tw}	Blade twist	-6°

In order to ensure a balance between the accuracy of modeling the rotor wake and the required computational resources, the calculated time step corresponding to the rotation of the rotor blade by 4 degrees in azimuth has been used. Each one of the calculated modes has been modeled for the number of revolutions of the rotor n = 16-24. With these settings for calculating a single mode, it has taken on average about 7 days work of a high-performance personal computer equipped with a central processor unit with eight computing cores (16 threads).

III. Results and Discussion

The first part of the paper has been dedicated to the validation of the applied free wake model in hover.

Figure 3 represents the performance diagram c_T=f(c_Q) for hover without ground effect. The calculation results coincide well with the available experimental data [24].

Figure 4 demonstrates the dependence of the main rotor thrust ratio on the ground effect $c_T/c_{T\infty}$ (H/R). The obtained result has been compared with the available experimental and calculated data [1], [9], [12], [13], [17], [19], [22], [23], [26] (Fig. 4). The presented calculation results are also in good agreement with the specified data.

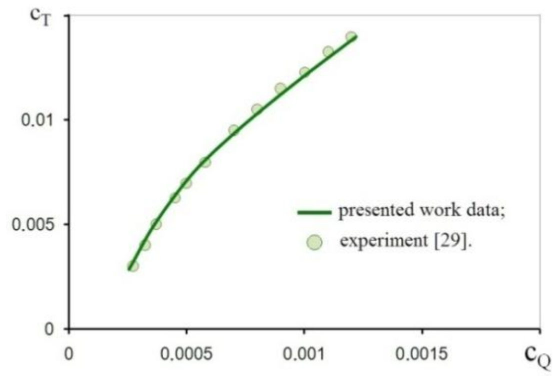

Fig. 3. Calculated and experimental [24] rotor performance diagrams in hover

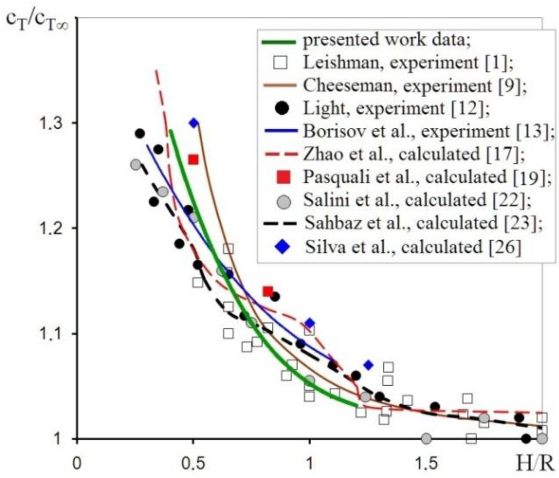

Fig. 4. Calculated and experimental diagrams of rotor thrust ratio in ground effect (c_Q = const)

The main part of the work is focused on modeling the main rotor aerodynamics in forward flight mode (hover at different wind speeds). In order to study the parameters of the rotor wake and the induced velocity fields under various conditions, a grid of calculated modes has been used. Parameter H, which determines the distance from the rotor hub to the ground surface, has varied in the range of H = 6-16 m (H = 6; 8; 10; 12; 16 m). The case of the main rotor operating out of ground effect ($H = \infty$) has been also considered. The flight speed (intensity of the wind) has been in the range of $V = 0{-}15$ m/s (V = 0; 5; 7.5; 10; 12.5; 15 m/s). The angle of attack of the rotor has been assumed to be $\alpha_R=0°$. The blade pitch angle of the main rotor has been chosen due to the condition of ensuring a constant rotor thrust equal to the take-off weight of the helicopter 13000 kg (c_T = 0.0127).

Thus, 36 rotor-operating modes have been calculated.

III.1. Main Rotor Wake and Flow Analysis in Ground Effect

Below, there are the results of visualization of the rotor wake shapes and the flow pictures using streamlines, obtained for the calculated operating modes.

Figures 5 show the results of the visualization of the main rotor wake shapes for the case of flying in ground effect at the fixed value of H = 8 m (H/R = 0.0563) at different forward flight speed values: V = 0; 5; 7.5; 10; 12.5 and 15 m/s. In Figures 6, streamlines are constructed in the OXY plane, which allows analyzing the character of the flow around the rotor on mentioned regimes. It can be seen that the ground effect significantly affects the formation of the rotor wake structures. At a certain distance from the rotor, the so-called "ground vortex" structure begins to form due to increasing speed of the incoming flow. It is clearly visible in the visualization of the rotor wake in Fig. 5(b) (V = 5 m/s), Fig. 5(c) (V = 7.5 m/s) and Fig. 5(g) (V = 10 m/s), as well as in the corresponding streamlines in Figures 6(b), 6(c) and 6(g). This phenomenon is well known and described in the literature, including the book by Leishman (2006) [1], studied through experimental methods (PIV) in the work by Nathan and Green (2012) [15], through calculation in the work by Brown and Whitehouse (2004) [22], Phillips (2010) [4] and Sugiura et al. (2017) [21]. Figure 5(b) shows that "ground vortex" arises as a result of rolling-up the leading edge of the rotor wake when flying at low speeds in ground effect and makes a significant feature in the velocity field around the rotor. It is seen that at V = 5 m/s V = 7.5 m/s "ground vortex" is located at a distance 2R from the rotor, and with increasing velocity to V = 10 m/s "ground vortex" is coming close to the rotor plane (Figs. 6).

Further, at V = 12.5 m/s it moves directly below the rotor (Fig. 6(d)). After passing under the rotor, it disappears. Fig. 6(e) shows that at V = 15 m/s, the "ground vortex" is no longer observed. At the same time, at V = 12.5 m/s (Fig. 5(d)), the formation of the right and left "supervortex" structures is observed. However, this happens in ground effect later than out of it (the formation of "supervortex" structures are observed starting from the velocity value of V = 7.5 m/s). The results of the main rotor wake and flow pictures' visualization in Figs. 5 and Figs. 6 show that in some specific cases, the tail rotor location may be close to the observed "ground vortex", which may affect its aerodynamic characteristics. It is also important to note that the "supervortexes" along the edges of the main rotor wake at V = > 12.5 m/s differ in their structure and position from the case of flying in ground effect. This means that for the same values of the forward flight speeds V (or equal wind speeds), the influence of the main rotor on the tail rotor for the cases of in/out of ground effects may differ significantly. Figures 7 and Figures 8 show the results of the main rotor wake and flow visualizations for a fixed flight speed value V = 10 m/s and different heights above the ground H = 6; 8; 10; 12; 16 m, as well as for the "off-ground" case ($H = \infty$).

From Figs. 7, it follows that at a fixed value of V = 10 m/s with a decrease in the distance to the ground surface H, the structure of the rotor wake has significant changes. "Supervortexes" changes their spatial position under the influence of the ground effect. At values of H = 16; 12 m (Figs. 7(b), (c)), left and right "supervortexes" expand and deviate to the left and right correspondingly. At H = 10 m, "supervortexes" begin to erode (Fig. 7(d)). At H = 8 m, the "supervortexes" are no longer observed. It is important to note that at the flow rate V = 10 m/s (μ = 0.0467) the ground effect almost does not affect the aerodynamic characteristics of the rotor, such as thrust and torque. However, the observed changes in the rotor wake structure can significantly affect the aerodynamic interference between the main and tail rotors. Therefore, at a low values of H = 6; 8 m tail rotor cannot get under the induced influence of main rotor "supervortex" structures because of their absence. At the same time, as follows from the streamlines presented in Figs. 8, at the values of H = 10; 8; 6 m, a "ground vortex" structure appears (Figs. 8(d), (e), (f)). Thus, taking into account the specificity of the rotor wake structure in ground effect, it is especially important when analyzing its potential induced effect on the tail rotor.

III.2. Analysis of Induced Velocity at the Tail Rotor Location Area

The presented results have been obtained for an isolated main rotor. The tail rotor has not been considered. This is the reason why the immediate influence of the main rotor on the aerodynamic characteristics of the tail rotor has not been evaluated. At the same time, it is possible to estimate the potential induced effect of the main rotor wake on the tail rotor. In order to achieve this goal, it is necessary to calculate and analyze the induced velocities in the tail rotor location area. Evidently, this task is rather complicated, because the position of the tail rotor location area relative to the main rotor wake may change due to hover under different wind directions or flying with slide.

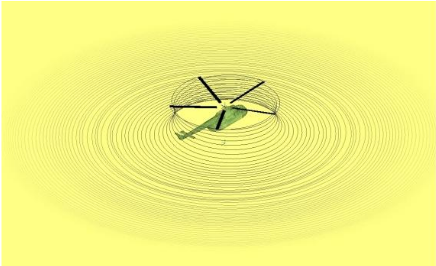

(a) V = 0 m/s

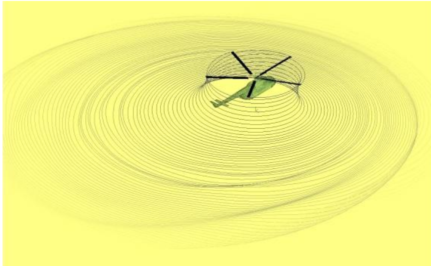

(b) V = 5 m/s

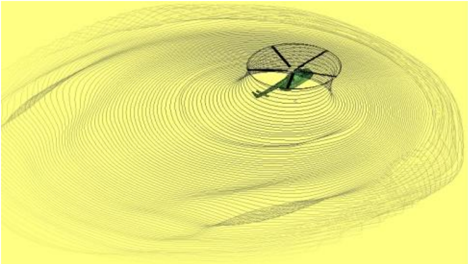

(c) V = 7.5 m/s

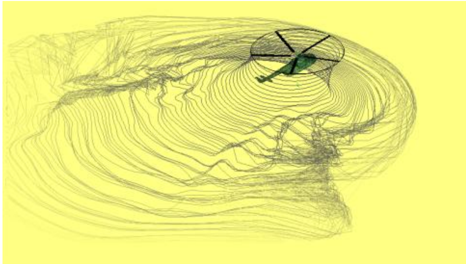

(d) V = 10 m/s

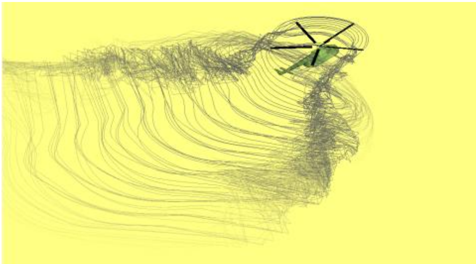

(e) V = 12.5 m/s

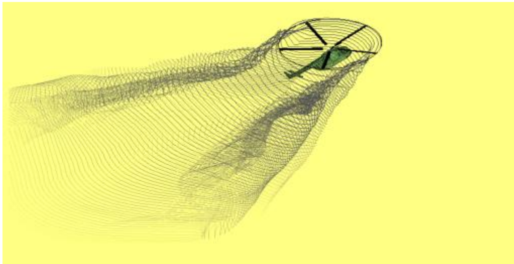

(f) V = 15 m/s

Figs. 5. Main rotor wake shape visualizations at the H = 8 m and V = 0−15 m/s

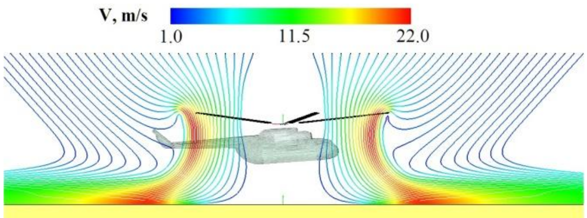

(a) V = 0 m/s

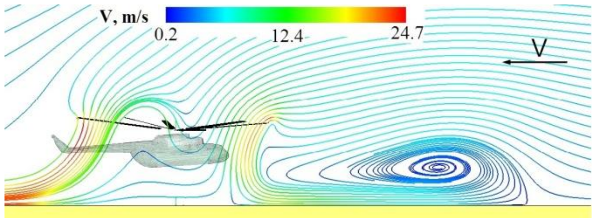

(b) V = 5 m/s

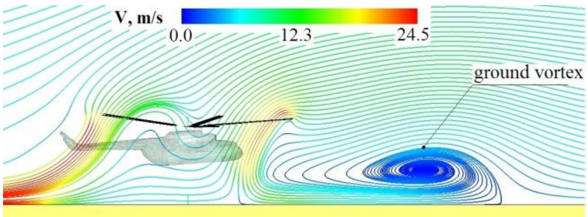

(c) V = 7.5 m/s

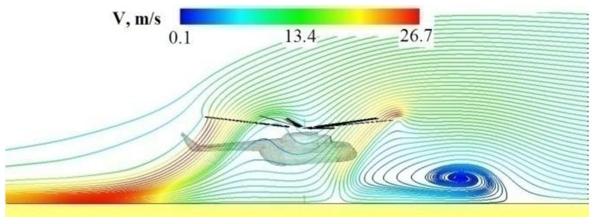

(d) V = 10 m/s

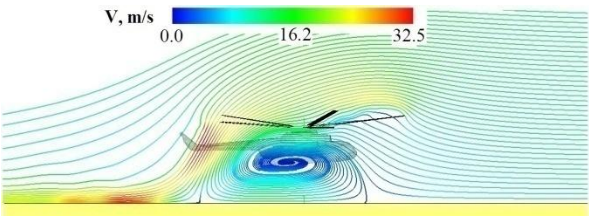

(e) V = 12.5 m/s

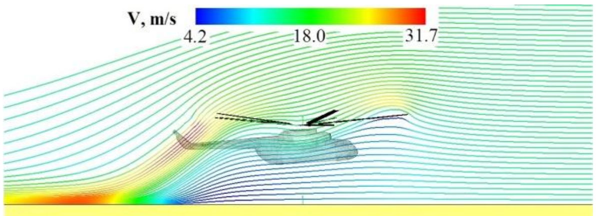

(f) V = 15 m/s

Figs. 6. Flow visualizations using streamlines at the H = 8 m and V = 0−15 m/s

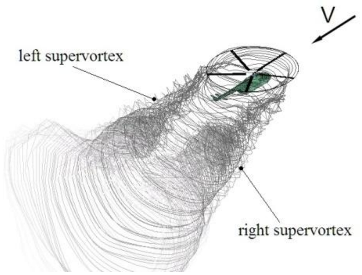

(a) H = ∞

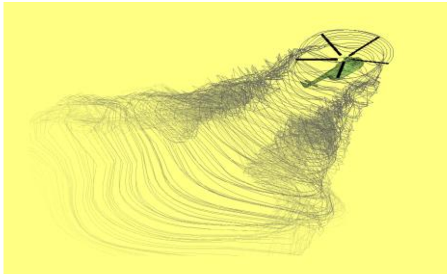

(b) H = 16 m

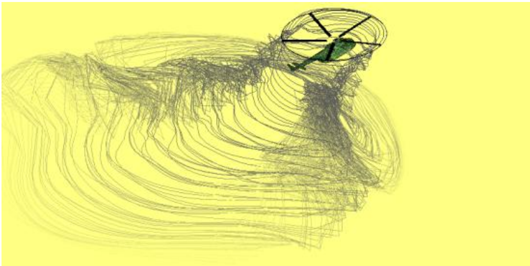

(c) H = 12 m

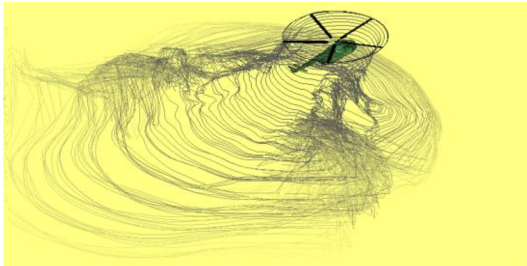

(d) H = 10 m

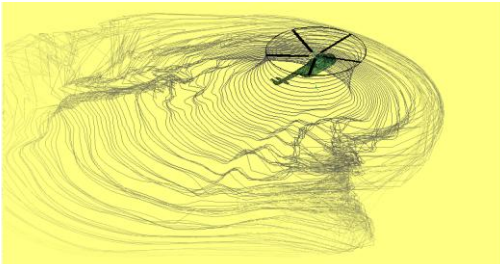

(e) H = 8 m

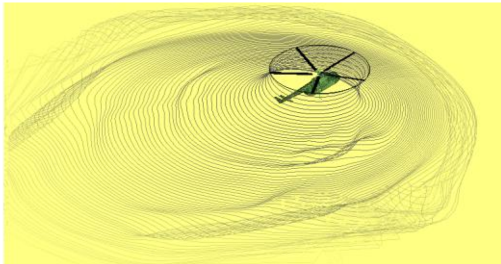

(f) H = 6 m

Figs. 7. Main rotor wake shape visualizations at the V = 10 m/s and H = 6−16 m; H = ∞

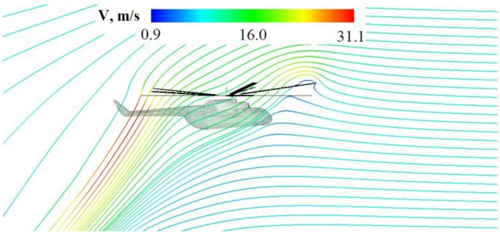

(a) H = ∞

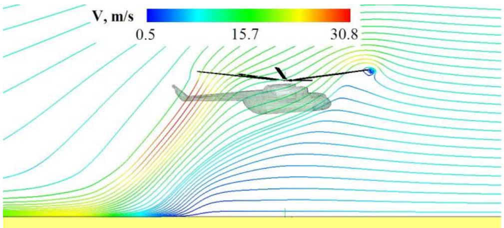

(b) H = 16 m

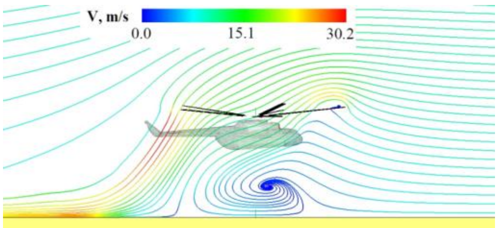

(c) H = 12 m

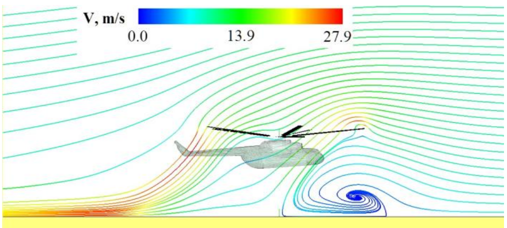

(d) H = 10 m

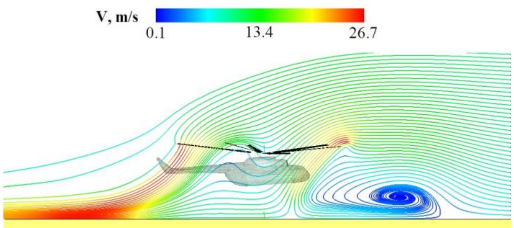

(e) H = 8 m

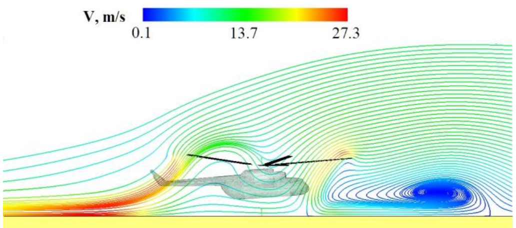

(f) H = 6 m

Figs. 8. Flow visualization using streamlines at the V = 10 m/s and H = 6−16 m; H = ∞

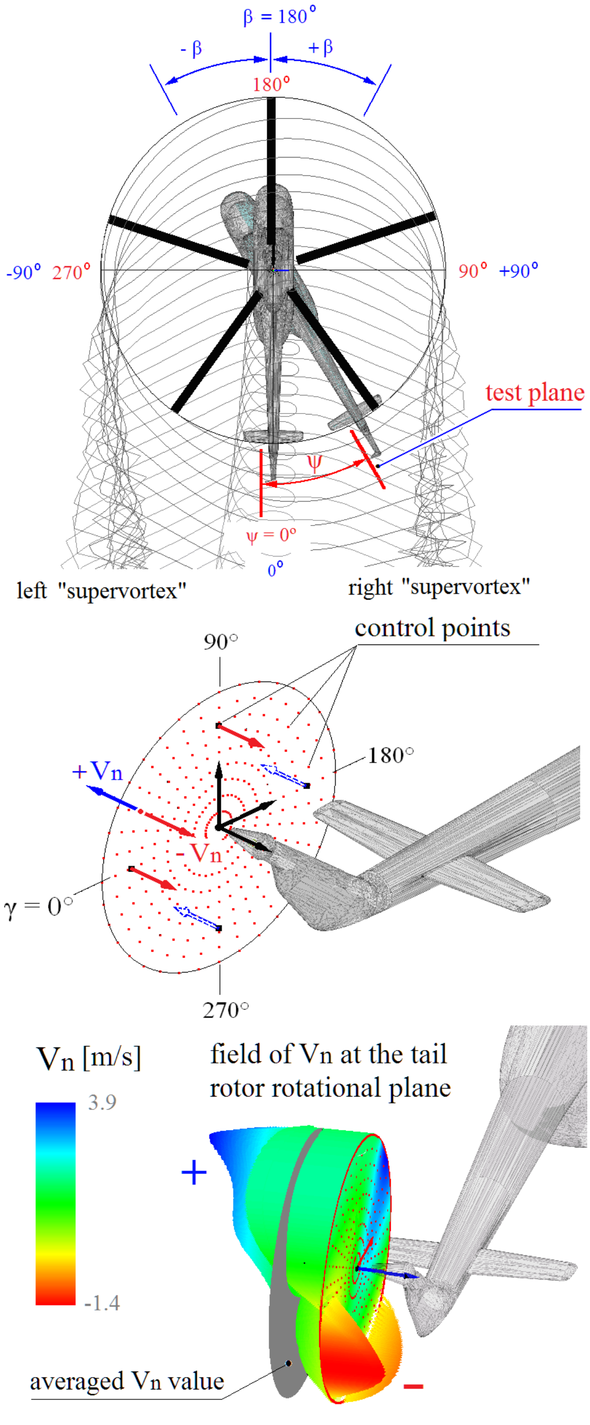

Fig. 9. Scheme of the test plane with control points for induced velocity fields' analysis

In order to calculate the induced velocity field in the tail rotor rotational plane, a test plane with an array of control points has been used (Fig. 9). The center of the test plane coincides with the center of the tail rotor hub.

The test plane contains 360 control points distributed evenly over the radius (10 points) and azimuth (36 points). The test plane may be rotated relatively to the main rotor axis from the initial position ψ = 0° with a step of $\Delta\psi$ =10º. Thus, for each calculated case there is an array of data describing the fields of inductive velocities in the plane of rotation of the tail rotor. The correspondence between the test plane rotation angles ψ and the angles slide β is shown in Fig. 9. In this paper, the normal components of the induced velocity V_n at control points, which have the greatest influence on the operating conditions of the tail rotor, are analyzed. The accepted rule of signs of the V_n is also shown in Fig. 9.

Figs. 10 show the diagrams of the induced velocity V_n averaged over the test plane (Fig. 9) for various angles of slide β and rotation angle ψ for different values of V. Diagrams are constructed for out of ground effect and for different distances H = 6; 8; 10; 12; 16 m. The values of V vary within V = 0−15 m/s. The tail rotor of the considered helicopter works at angles ψ = 0−180° with the positive angles of attack, and at angles ψ = 180-360° with the negative angles of attack. The presented diagrams show that the greatest induced effect from the main rotor wake to the tail rotor rotational plane is observed at the angles of slide β = 30−90º and in the range from β =-30° to β =-90°. At these angles of slide, the tail rotor is affected by the right and left "supervortexes" of the main rotor wake. As shown above, the presence of the ground surface at low values of H (especially at H = 6; 8 m) significantly affects the structure of the main rotor wake. At V = 7.5 and 10 m/s with a decrease of H, the values of the averaged induced velocity in the plane of tail rotor rotation fall by 2−3 times. At V = 12.5 and 15 m/s, such a decrease is not observed, this fact indicates "supervortex" structures in these modes even at low values of H. Thus, the values of V = 7.5 and 10 m/s are the most typical in terms of the influence of distance H on main rotor wake structure. In these modes, when the H value changes from 10 to 16 m, the values of the average induced velocity in the tail rotor plane may in some cases change by 2-3 times, which can significantly affect the working conditions and aerodynamic characteristics of the tail rotor.

IV. Conclusion

Based on the free wake model developed at the Helicopter Design Department of Moscow Aviation Institute, a numerical modeling of the aerodynamic characteristics of an isolated main rotor of Mi-8 single-rotor helicopter in ground effect has been performed. The math model of isolated rotor at hover in ground effect has been verified by comparing the obtained data with the results of experimental and computational studies by other authors. The presented calculations have been made for the values of distance from the ground surface to the rotor hub: H = 6; 8; 10; 12; 16 m, and for the case of out of ground effect flight: $H = \infty$. For each one of these H values, the flight speed (wind speed in hover) values of V= 0; 5; 7.5; 10; 12.5; 15 m/s are considered. The rotor thrust has been a constant value and equal to the take-off weight of the helicopter 13000 kg. As a result of conducted research, it has been found out that the proximity of the ground surface has a significant impact on the structure of the rotor wake.

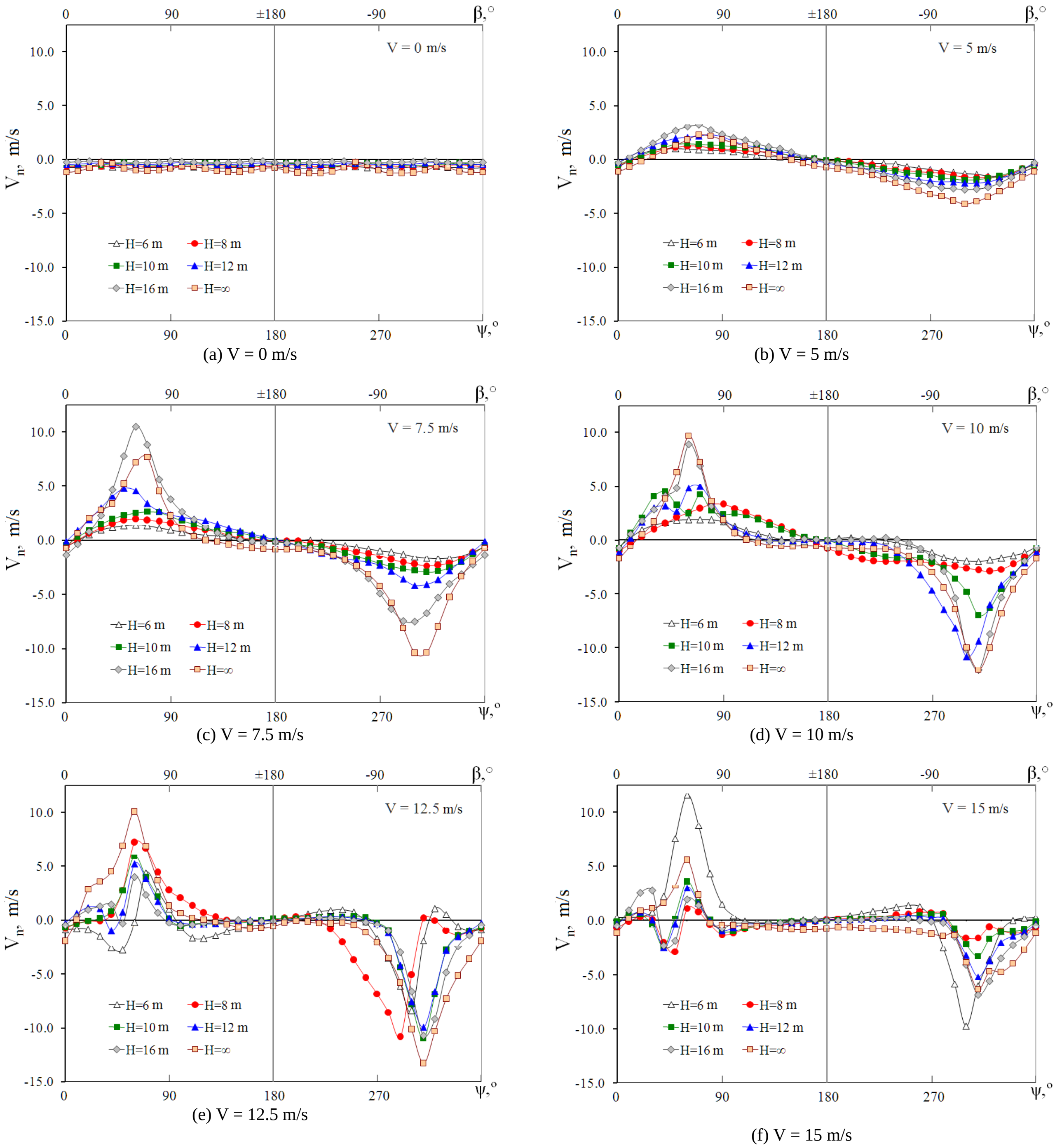

Figs. 10. Calculated diagrams of the induced velocity Vn averaged over the tail rotor rotational plane for various angles of slide β and free stream velocity values V

At the low values of H = 6 and 8 m and values of V = 7.5 and 10 m/s, there are no "supervortex" structures observed in these modes in case of out of ground effect ($H = \infty$). At the same time, the "ground vortex" structure is observed. At high values of V and H, "supervortex" structures are formed, but they have a different location (compared to $H = \infty$). It has been found out that at flight speeds V = 7.5 and 10 m/s, the velocity field in the area of the tail rotor location at the same angles of slip significantly depends on the distance above the ground H. In particular, when the value of H decreases from 16 to 8 m, the value of the averaged induced velocity in some cases decreases by 3-4 times. The presented results confirm the importance of the ground effect when determining the induced effect of the main rotor on the tail rotor at different flight speeds and angles of slip. The obtained data on the induced effect of main rotor wake in the area of the tail rotor location have been used to refine the simplified mathematical model of helicopter flight simulator of JSC Helicopters Mil and Kamov. The presented research can be developed in numerical simulation of the combination of the main and tail rotors in ground effect, with taking into account aerodynamic interference. This will allow evaluating the influence of studied effects on the tail rotor thrust values.

References

[1] J. G. Leishman, *Principles of Helicopter Aerodynamics*. (Cambridge University Press, 2000).

[2] Yu. M. Ignatkin et al, Research Of Vortical Wake Structure For Main Rotor Of Helicopter On Low Flight Speeds, *All-Russian Scientific-Technical Journal "Polyot"*, No. 3, 2018, pp. 52-59. (In Russian).
http://www.ros-polet.ru/index_EN

[3] Y. Ignatkin et al, Modelling the helicopter rotor aerodynamics at forward flight with free wake model and URANS method. *Aviation*. 24, No. 4, 2020, pp. 149-156.
doi:https://doi.org/10.3846/aviation.2020.12714

[4] C. Phillips, *Computational study of rotorcraft aerodynamics in ground effect and brownout*. Ph.D. dissertation, University of Glasgow, UK, 2010.
https://theses.gla.ac.uk/1783/

[5] T. Fletcher, R. E. Brown, Helicopter tail rotor thrust and main rotor wake coupling in crosswind flight, *Journal of Aircraft*, Vol. 47, 2010, pp. 2136-2148.
doi: 10.2514/1.C031018

[6] Yu. M. Ignatkin et al, Computational modeling of interference between helicopter main and tail rotors based on nonlinear blade vortex model. *Russian Aeronautics*, Vol. 59, 2016, pp. 44-50.
doi: 10.3103/S1068799816010074

[7] Yücekayali, Arda & Ortakaya, Yüksel. Viscous Vortex Particle Method Explored for Main Rotor-Tail Rotor Interaction, *The 8th Asian/Australian Rotorcraft Forum*, (2019).

[8] M. Knight, R. A. Hefner, *Analysis of Ground Effect on the Lifting Airscrew*, NASA TN-835, (1941).

[9] I. C. Cheeseman, W. E. Bennett, *The Effect of the Ground on a Helicopter Rotor in Forward Flight*, R & M 3021, Aeronautical Research Council, (1957).

[10] J. Koo, T. Oka, *Experimental Study on the Ground Effect of a Model Helicopter Rotor in Hovering*, NASA TT-F-13938, (1971).

[11] P. F. Sheridan, W. Wiesner, Aerodynamics of helicopter flight near the ground. *The 33th annual forum of the American helicopter society*, (1977).

[12] J. Light, Tip vortex geometry of a hovering helicopter rotor in ground effect, *Journal of the American Helicopter Society*, Vol. 38, No. 2, 1993, pp. 34-42.
doi: https://doi.org/10.4050/JAHS.38.34

[13] E. A. Borisov et al, Experimental research of influence of sites size restrictions on aerodynamic characteristics of the rotor, *Civil Aviation High Technologies*, No. 212, 2015, pp. 98-104. (In Russian).
https://avia.mstuca.ru/jour/issue/archive

[14] T. Lee, J. G. Leishman, M. Ramasamy, Fluid dynamics of interacting blade tip vortices with a ground plane, *Journal of The American Helicopter Society*, Vol. 55, 2008, pp. 22005-2200516.
doi: 10.4050/JAHS.55.022005

[15] N. D. Nathan, R. B. Green, The flow around a model helicopter main rotor in ground effect. *Exp Fluids*, Vol. 52, 2012, pp. 151-166.
doi: 10.1007/s00348-011-1212-1

[16] A. D. Griffiths, J. G. Leishman, A Study of Dual-Rotor Interference and Ground Effect Using a Free-Vortex Wake Model, *The 58th Annual Forum and Technology Display of the American Helicopter Society*, 2002, pp. 592–612.

[17] J. Zhao, C. He, Physics – Based Modeling of Viscous Ground Effect for Rotorcraft Applications. *The 70th annual forum of the American helicopter society*, (1977).

[18] A.A. Aparinov et al, Numerical modeling of helicopter main rotor behavior near a small-scale helideck by the vortex method. *Russian Aeronautics*, Vol. 60, 2017, pp. 500-507.
doi: 10.3103/S1068799817040043

[19] C. Pasquali et al, Numerical-experimental correlation of hovering rotor aerodynamics in ground effect, *Aerospace Science and Technology*, Volume 106, 2020.
doi: 10.1016/j.ast.2020.106079

[20] B. M. Kutz et al, Numerical investigation of helicopter rotors in ground effect, *The 30th AIAA Applied Aerodynamics Conference*, (2012).
doi:10.2514/6.2012-2913

[21] M. Sugiura et al, Validation of CFD Codes for the Helicopter Wake in Ground Effect, *The 43th European Rotorcraft Forum*, (2017).

[22] N. Salini et al, An Evaluation of Ground Effect Modelling for Rotors in Hover. *The 6th Asian/Australian Rotorcraft Forum*, (2017).

[23] Şahbaz, Mehmet & Sezer Uzol, Nilay & Kurtulus, Dilek, Numerical and Experimental Investigation of Rotor Aerodynamics In Ground Effect with Inclined Planes, *The 8th Asian/Australian Rotorcraft Forum*, (2019).

[24] F. Rovere et al, CFD Analysis of a micro rotor in ground effect, *The 45th European Rotorcraft Forum*, (2019).
doi: https://doi.org/10.2514/6.2020-1793

[25] X. Wang et al, Research on Finite Ground Effect of a Rotor, *The IEEE/RSJ International Conference on Intelligent Robots and Systems (IROS)*, (2019),
doi: https://doi.org/10.1109/IROS40897.2019.8968083

[26] P. Silva et al, Simple multiple reference frame for high-order solution of hovering rotors with and without ground effect, *Aerospace Science and Technology*, Volume 111, 2021, 106518
doi: https://doi.org/10.1016/j.ast.2021.106518

[27] R. E. Brown, G. R. Whitehouse, Modelling Rotor Wakes in Ground Effect. *Journal of the American Helicopter Society*, Vol. 49, 2004, pp. 238-249.
doi:10.4050/jahs.49.238

[28] Yu. M. Ignatkin et al, A Nonlinear Blade Vortex Propeller Theory and Its Applications to Estimate Aerodynamic Characteristics for Helicopter Main Rotor and Anti-Torque Rotor, *Vestnik MAI*, Vol. 16, No. 5, 2009, pp. 24-31. (In Russian).
http://vestnikmai.ru/eng/publications.php?ID=12351&eng=Y

[29] V. B. Zozulya, Y. P. Ivanov, *Practical Aerodynamics of Mi-8 Helicopter*, (Mashinostroenie, Moscow, 1977). (In Russian).

[30] Marchetto, F., Benini, E., Numerical Simulation of Harmonic Pitching Supercritical Airfoils Equipped with Movable Gurney Flaps, (2019) *International Review of Aerospace Engineering (IREASE)*, 12 (3), pp. 109-122.
doi: https://doi.org/10.15866/irease.v12i3.16723

[31] Sugar-Gabor, O., Numerical Study of the Circular Cylinder in Supersonic Ground Effect Conditions, (2018) *International Review of Aerospace Engineering (IREASE)*, 11 (1), pp. 15-26.
doi: https://doi.org/10.15866/irease.v11i1.13696

[32] Sunil, A., Tide, P., Numerical Investigations on Suppression of Aeolian Vibrations on a Tall Chimney Using Helical Strakes, (2019) *International Journal on Engineering Applications (IREA)*, 7 (5), pp. 152-159.
doi: https://doi.org/10.15866/irea.v7i5.17764

Authors' information

[1]Moscow Aviation Institute (National Research University), Moscow, Russia.

[2]JSC Helicopters Mil & Kamov, Moscow region, Russia.

Yuri M. Ignatkin is Ph.D of Engineering Sciences, Associate professor at the Helicopter Design Department of the Moscow Aviation Institute (National Research University). Research interests include experimental aerodynamics, computational fluid dynamics and helicopter aerodynamics.
E-mail: IgnatkinYM@mai.ru

Pavel V. Makeev is Ph.D of Engineering Sciences, Associate professor at the Helicopter Design Department of Moscow Aviation Institute (National Research University). Research interests include computational fluid dynamics and helicopter aerodynamics.
E-mail: MakeevPV@mai.ru

Alexander. I. Shomov is Ph.D of Engineering Sciences, Associate professor at the Helicopter Design Department of Moscow Aviation Institute (National Research University). Research interests include aerodynamics and helicopter design.
E-mail: Shomov_Aleksandr@mail.ru

Valery A. Ivchin is Ph.D of Engineering Sciences, Deputy chief designer of the JSC Helicopters Mil & Kamov, Moscow region, Russia. Research interests include helicopter aerodynamics, dynamics and helicopter design.
E-mail: valivchin@mail.ru